1970

An experimental and theoretical study of the nucleation of water vapor on ions in helium and argon

Daniel R. White
Missouri University of Science and Technology

Department: Physics

AN EXPERIMENTAL AND THEORETICAL STUDY OF THE NUCLEATION OF WATER VAPOR ON IONS IN HELIUM AND ARGON

A Dissertation

Presented to

the Faculty of the Graduate School

University of Missouri - Rolla

In Partial Fulfillment

of the Requirements for the Degree

Doctor of Philosophy

---

by

Daniel Ralph White

September 1970

James L. Kassner, Jr., Dissertation Supervisor

AN EXPERIMENTAL AND THEORETICAL STUDY OF THE NUCLEATION OF WATER VAPOR ON IONS IN HELIUM AND ARGON

by

DANIEL RALPH WHITE, 1940 -

A DISSERTATION

Presented to the Faculty of the Graduate School of the

UNIVERSITY OF MISSOURI - ROLLA

In Partial Fulfillment of the Requirements for the Degree

DOCTOR OF PHILOSOPHY

in

Engineering Physics

1970

James L. Kassner Jr.
Advisor

Kevin V. Lund

J. W. Rivers

David N. Montgomery

A. J. Panico

AN EXPERIMENTAL AND THEORETICAL STUDY OF THE NUCLEATION OF WATER VAPOR ON IONS IN HELIUM AND ARGON

An Abstract of a Dissertation

Presented to

the Faculty of the Graduate School

University of Missouri - Rolla

In Partial Fulfillment

of the Requirements for the Degree

Doctor of Philosophy

---

by

Daniel Ralph White

September, 1970

AN EXPERIMENTAL AND THEORETICAL STUDY OF THE NUCLEATION OF WATER VAPOR ON IONS IN HELIUM AND ARGON

Abstract

The nucleation of water vapor on ions in atmospheres of helium and argon was studied using an expansion type cloud chamber. Separation of the positive and negative ions was achieved so that the nucleation could be studied as a function of both the sign of the ionic charge and the supersaturation.

A semiphenominological theory was developed as an extension of the classical theory to include the effects of the ionic charge on the nucleation process. The theoretical model of the prenucleation embryo was assumed to possess an oriented dipole surface layer with the direction of orientation dependent on the sign of the ionic charge. The theory predicts not only the increase in the nucleation rate compared to that for homogeneous nucleation and a difference in rate between positive and negative ions, the negative ions having the higher nucleation rate, but also predicts a correction term to the classical theory of homogeneous nucleation for polar molecules which exhibit an electrical double layer at the liquid surface.

Comparisons between the experimental and theoretical results for homogeneous nucleation, and nucleation on both positive and negative ions were made and the results used to draw some conclusions as to the possible structure of the prenucleation embryo.

ACKNOWLEDGMENTS

The author would like to express his gratitude to his advisor, Dr. James L. Kassner, Jr., for his advice and assistance during the course of this research. Thanks are also due to Dr. Neville H. Fletcher and Dr. William J. Dunning for the encouragement and suggestions resulting from discussions with them.

Especial thanks are due to Paul Yue for the many hours he spent assisting in preparing the equipment and collection of the experimental data; and to Arthur Biermann for his advice in preparing computer programs used in various aspects of the work. Thanks are also due to the many students, both past and present, who have contributed to bringing the cloud chamber used in this work to its present state of refinement.

The author's wife, Bernice, deserves especial thanks for her continuous encouragement and patience during our years in school.

The author is indebted to the Department of Health, Education and Welfare for their support during part of his program. The work was supported by the Atmospheric Sciences Section, National Science Foundation, NSF Grant GA-1501.

TABLE OF CONTENTS

LIST OF FIGURES

LIST OF TABLES

I. INTRODUCTION

The basic processes governing the formation and development of clouds are the microphysical processes active in the creation and development of the individual droplets.[1] At present these processes are only poorly understood, the heterogeneous nucleation process being complicated by the presence of a foreign particle, normally possessing unknown composition and surface properties. Much of the past theoretical and experimental work of this laboratory has been directed towards an understanding of homogeneous nucleation. While it does not occur in the atmosphere, it is the simplest form of nucleation and provides a foundation for understanding the more complex heterogeneous case.

The classical liquid drop model of homogeneous nucleation as developed by Volmer and Weber,[2] Farkas,[3] Becker and Doring,[4] Frenkel[5] and Zeldovich,[6] while understandably inadequate, probably provides the most convenient basis for extension to the simplest of the heterogeneous cases, namely, nucleation on ions. The choice of ions, as a first step in considering heterogeneous nucleation, is logical since it does not introduce the poorly characterized properties of a foreign particle into the problem. Moreover, the ion itself is of the same order of magnitude in size as the condensing vapor molecules. The field due to the ion's charge, however, does introduce additional interactions into the problem, by its interaction with the molecules of the prenucleation embryo, particularly with those in the surface of the embryo. Therefore, it would appear that a study of nucleation rates on ions would provide additional insight into the structure of the prenucleation embryo.

With this in mind a theoretical model has been developed for nuclea-

tion on ions, based on an extension of the liquid drop theory.

In the absence of electric fields many polar substances exhibit an electric double layer at their surface. The dependence of the surface structure on the direction of the ionic field introduces a sign dependent term in the free energy of formation of the embryo, a feature not included in previous theoretical models.[7-11] As a test of the theory, nucleation rates of water vapor on ions were measured experimentally using an expansion cloud chamber and comparisions made between the predictions of the theory and the experimental results.

II. EXPERIMENTAL METHOD

Experimental methods used in the study of homogeneous nucleation range from the steady state determination of the critical supersaturation as a function of temperature using diffusion cloud chambers, for example Katz and Ostermier,[12] to the measurement of extremely high nucleation rates using nozzles, for example Wegener,[13] and Wegener and Pouring.[14] However, these two extremes are unsuited for measuring nucleation rates on ions. The diffusion cloud chamber with its steady state operation makes the measurement of nucleation rates as a function of saturation all but impossible, and the separation of positive and negative ions is difficult and uncertain. The large drop densities required for measurements in nozzle experiments completely masks the effects on nucleation rates due to any ions present and the large quantities of carrier gas makes complete removal of aerosol contaminates unlikely. The expansion cloud chamber, as developed by Allen and Kassner,[15] is well suited to the measurement of nucleation rates on ions. The peak supersaturation of the chamber, shown in Figure 1, can be varied from 1.0 to greater than 7.0 by controlling the amount of air released from the volume under the piston. The chamber sensitive time can be varied from .01 seconds to approximately 1.0 second before heat flow from the walls make the results unreliable, and the initial temperature can be varied between approximately 15°C and 45°C.

The chamber was programmed to cycle automatically; one cycle consisted of four primary expansions each followed by an over-compression of the chamber and a secondary expansion which returned the chamber to the preexpansion pressure. The first three primary expansions of a cycle, see Figure 2A, yielded peak supersaturations

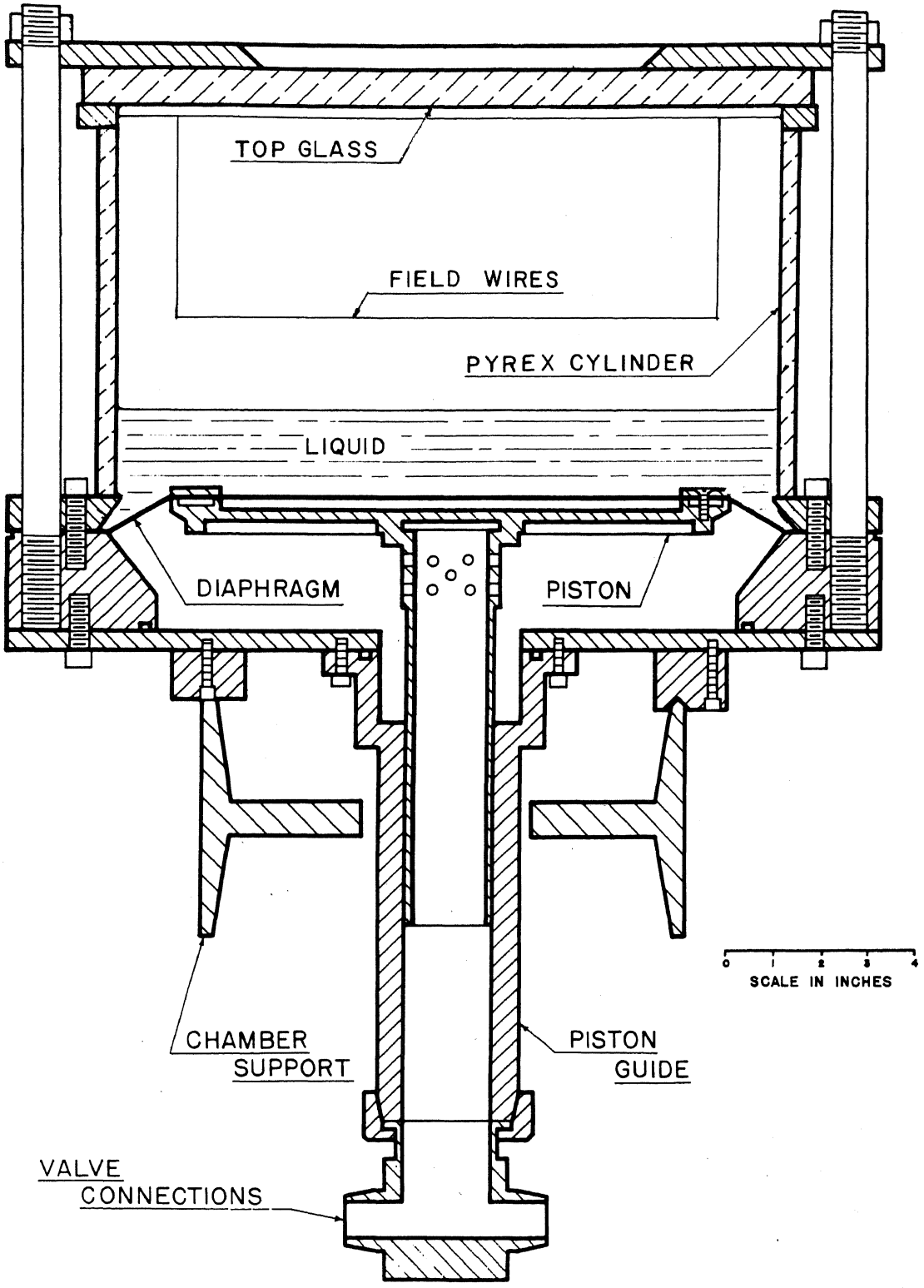

Figure 1. Diagram of expansion cloud chamber.

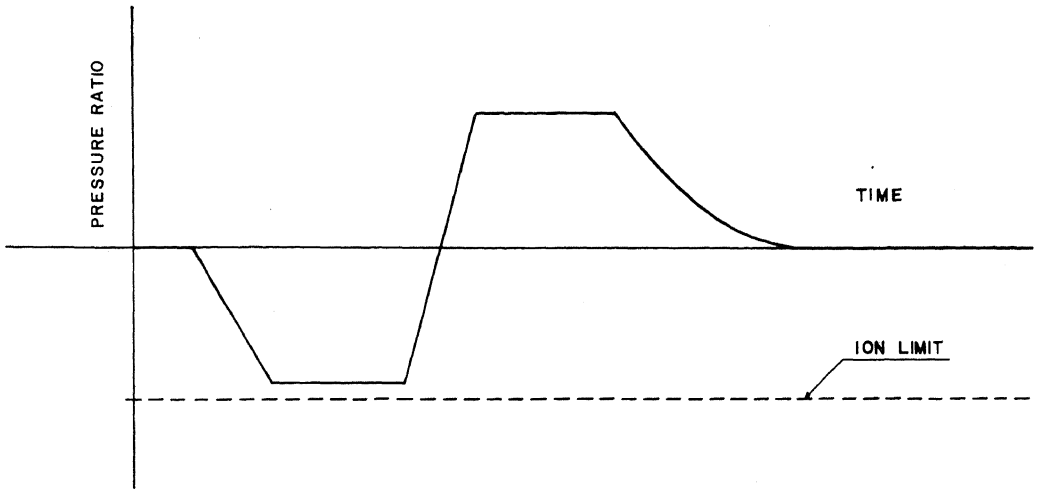

Figure 2A. Cleaning expansions.

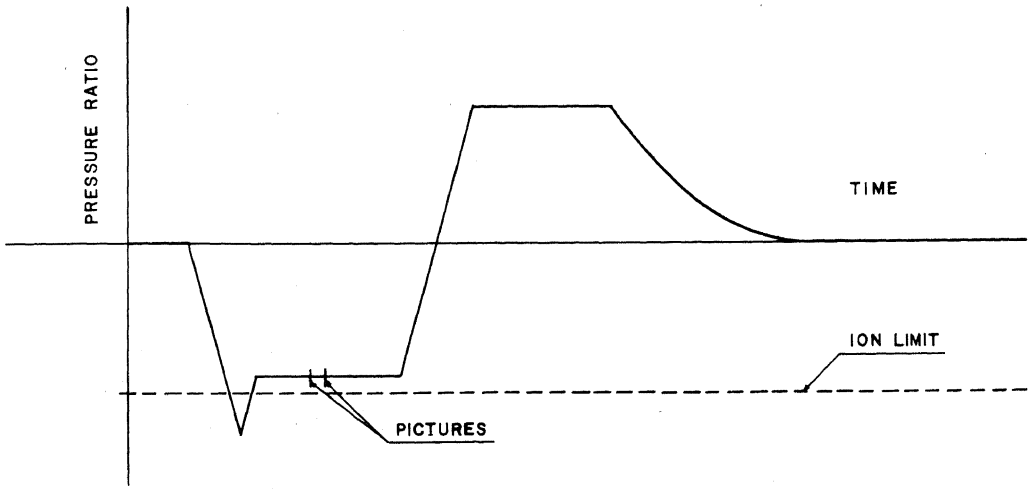

Figure 2B. Data expansions.

below the ion limit and were used to clear the chamber of any re-evaporation nuclei[16,17] left from previous expansions. The fourth primary expansion, see Figure 2B, was used for collection of data. Data expansions reached peak supersaturations which were varied from below the ion limit to well above the cloud limit. The primary data expansion was immediately followed by a small compression, which reduced the supersaturation to a value just below the ion limit. The partial compression effectively stopped any further nucleation yet permitted those drops already nucleated to grow to visible size.

After sufficient growth time two sets of stereo pictures were taken of the sensitive volume, at an interval of .07 seconds. The chamber then returned to the pre-expansion pressure in the same manner as the first three expansions, and the chamber automatically started a new cycle. The overall cycle time was approximately sixteen minutes. The photography utilized two flash lamps which produced light beams having well defined upper and lower limits; this permitted simple conversion from photographic area to chamber volume.

A pressure transducer and multichannel light beam ocillograph were used to obtain a continuous measurement of the pressure in the sensitive volume during the data expansions. The pressure data, together with the initial temperature, read from a thermocouple, and the equation of state for the carrier gas and water vapor mixture was then used to calculate the supersaturation as a function of time throughout the expansion. This technique was first developed by Kassner and Schmitt.[18]

The chamber was kept free of ions between expansions by an electric clearing field inside the sensitive volume. Just prior to the data expansion the electric field was turned off, the chamber irradiated

with a narrow beam of x-rays and the electric field turned on for a short time to separate the positive and negative ions formed by the x-rays. The chamber was then expanded and photographed. This procedure permitted study of the nucleation as a function of the sign of the ionic charge. The x-ray beam was monitored for each expansion to permit normalization of the drop density to the total ion density.

III. THEORY

A. Introduction

The classical liquid drop theory of homogeneous nucleation[2-6] begins by considering the difference in free energy, $\Delta\Phi_H$, between g molecules in the vapor state and the same number of molecules clustered into an embryo, given by

$$\Delta\Phi_H = -(\phi_A - \phi_B)g + 4\pi\sigma_o r^2 , \qquad (1)$$

where ϕ_A and ϕ_B are the chemical potentials of the molecules in the vapor and liquid states, r, the radius of the embryo and σ_o, the macroscopic surface free energy.

In recent years there has been a rather lengthy debate concerning corrections made by Lothe and Pound[19] to account for the rotational and translational energies of the embryo. The original correction caused the nucleation rate to be increased by a factor of 10^{17}, destroying the previous agreement between the liquid drop theory and experiment. Reiss et al.[20,21] among others have concluded that while there are corrections of this type required those made by Lothe and Pound are too large. Reiss et al. have shown that the correction, while related to the translational partition function, is not equal to it and there is no contribution from rotation; the resulting correction to the nucleation rate is a factor between 3×10^3 and 1×10^6 which is much smaller than the 10^{17} given by Lothe and Pound.

As indicated by Lothe and Pound and shown by Russell,[11] the magnitude of the Lothe-Pound correction is greatly reduced when applied to ions. This is due to assuming that the embryos grow from small stable hydration clusters instead of monomers as in homogeneous nucleation. This, together with the conclusions of Reiss et al., led

to a decision not to include a Lothe-Pound type correction in the present theory.

B. Theoretical Model

The model used in this work consists of a spherical droplet having an oriented dipole layer at the surface. The ion is assumed to be located at the center of the droplet, and the sign of the ionic charge determines the direction of orientation of the dipoles. Comparision of the dipole-ion interaction energy with the thermal energy indicates that the influence of the ion will predominate out to approximately 15 Å, which is larger than the predicted radius of the critical nucleus for conditions normally encountered in cloud chambers. This predominance is important because one sign of the ionic charge will cause the dipoles to assume an alignment opposite to that which occurs in a neutral droplet, see Figure 3.

Abraham,[22] based on comparision of the energies of ordered and disordered surfaces for small droplets, has concluded that for droplets smaller than a certain size, g_t, the surface is disordered, and for droplets larger than g_t the surface is ordered. g_t depends on both temperature and supersaturation and can be either smaller or larger than the critical nucleus. Abraham's work considers only the neutral droplet and in the present work the ion introduces an additional ordering influence which becomes stronger as the size of the droplet decreases. Therefore it is assumed that the influence of the ion is sufficient to cause ordering of the surface for the prenucleation embryos considered in this work.

The inclusion of an ion within the embryo and the presence of an oriented surface layer require additional terms to be added to the expression for the change in free energy of the embryo. Those consid-

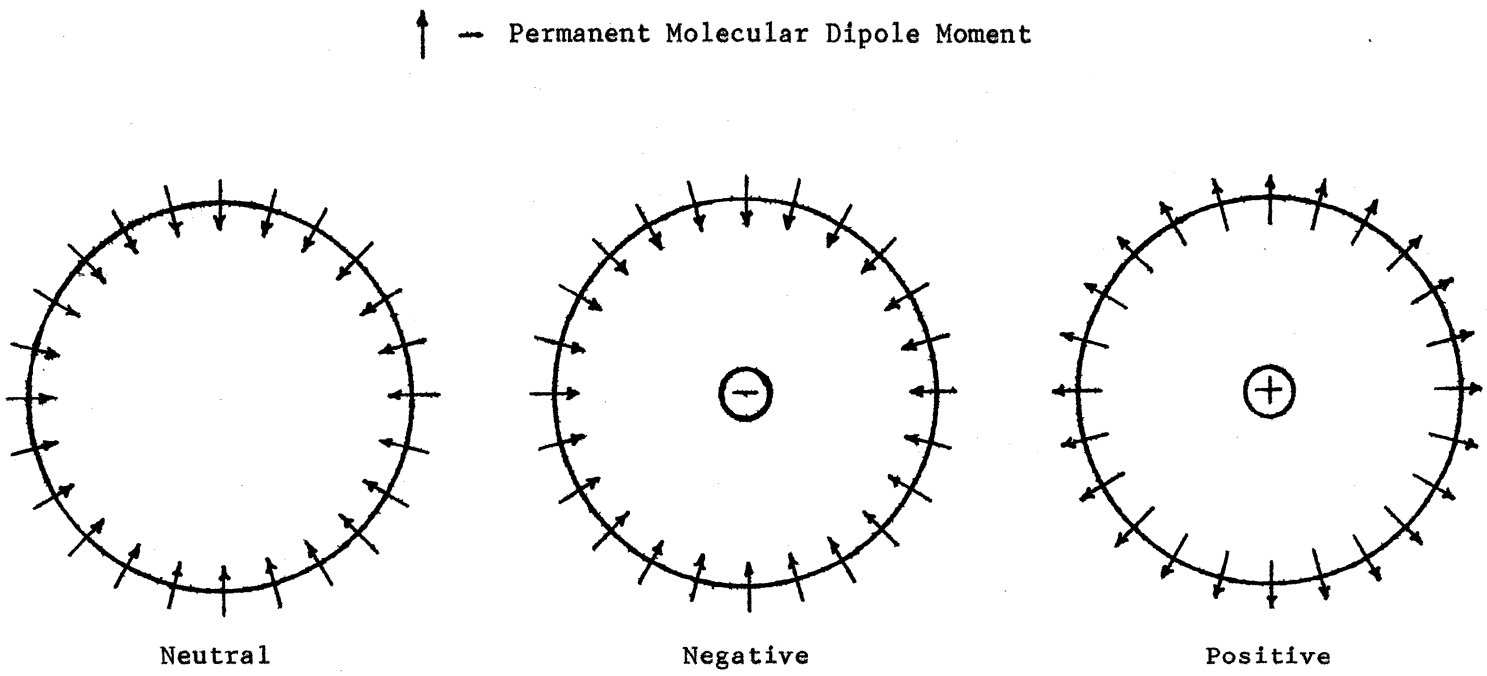

Figure 3. Surface Dipole Orientations.

ered in the present work are an electrostatic term for the bulk interaction of the ion with the surrounding liquid molecules, a dipole-dipole interaction to account for the nonparallel alignment of the surface dipoles due to the small radius of curvature of the surface and a dipole-quadrupole term due to the nonisotropic surroundings experienced by the surface molecules.

C. Electrostatic Correction Term

This term is basically the term considered by previous workers[5,7-11,23] to account for the effects of ions on the nucleation rate. The change in the electrostatic energy of the ions due to the presence of the embryo in general form is:

$$\Delta\Phi_{ES} = 1/8\pi\int_{\tau}\bar{D}_e \cdot \bar{E}_e d\tau - 1/8\pi\int_{\tau}\bar{D}_v \cdot \bar{E}_v d\tau \ , \qquad (2)$$

where the subscripts e and v refer respectively to the fields with and without the embryo present, and τ is the volume of the embryo. The integration is limited to the volume of the embryo because outside the liquid the two terms are identical and cancel. In the vapor $\bar{D}_v = \varepsilon_v\bar{E}_v$, and if it is assumed that $\varepsilon_v = 1$, then $D_v = E_v = \frac{e}{r^3} \cdot \bar{r}$ where $\bar{r}$ is the vector distance from the center of the ion (and embryo) and e is the ionic charge.

In the embryo $\bar{D}_e = \varepsilon_e\bar{E}_e$, and one of the main difficulties has been the choice of the value of ε_e that applies in the case of a small embryo. Assuming as a first approximation that ε_e is a scaler constant the change in electrostatic free energy is

$$\Delta\Phi_{ES} = 1/8\pi\int_{\tau}(\frac{1}{\varepsilon_e} - 1)D^2 d\tau = 1/8\pi\int_{r}^{r_e}(1 - \frac{1}{\varepsilon_e})\frac{e^2}{r^4}4\pi r^2 dr$$

$$= -\frac{e^2}{2}(1 - \frac{1}{\varepsilon_e})\ (\frac{1}{r_e} - \frac{1}{r}) \ , \qquad (3)$$

where r_e is the ionic radius, and ε_e, the effective dielectric constant

of the liquid.

Barring a dependence of ε_e on the sign of the ionic charge, (which at present seems unlikely), the electrostatic correction alone, while increasing the nucleation rate, is incapable of accounting for the sign dependence of the nucleation rate.

D. Dipole-Quadrupole Surface Correction Term

Frenkel[5] points out that consideration of only the dipoles of an oriented surface will not predict a sign preference, but including the quadrupole moment could account for the sign preference. This idea is supported by the results of Loeb et al.[24] and Good.[25] From an examination of the substances which show a sign preference and those that do not as listed by Loeb et al., one can easily see a direct correlation with the listing by Good of substances which have an abnormally low surface entropy and those which have a "normal" surface entropy. The first group has a low surface entropy, shows a sign preference, has permanent molecular electric dipole and quadrupole moments and tends to show a large degree of hydrogen bonding in the liquid state. The second group has a "normal" surface entropy, shows no sign preference, lacks either a permanent molecular dipole or quadrupole moment or both, and in general does not readily form hydrogen bonds. Both Good and Abraham[26,27] have attributed the low surface entropies of the first group to the presence of an ordered dipole surface layer.

Assuming the vapor-liquid surface to be composed of a layer of ordered dipole-quadrupole units, there exists an energy difference between the configuration in which all the dipoles are directed out of the liquid and the configuration in which they are all directed into the liquid. The procedure of Stillinger and Ben-Naim[28] will be used as a guide in obtaining an approximation for this energy difference.

Consider a set of Cartesian coordinates with the oxygen atom of a water molecule located at the origin and the hydrogen atoms lying in the y-z plane. Let the permanent dipole of the molecule be directed along the +z-axis, which also serves as the two-fold symmetry axis of the molecule. This choice of coordinates diagonalizes the quadrupole tensor of the molecule. To account for the inability of other molecules to penetrate the molecule fixed at the origin it is assumed to be surrounded by a sphere of exclusion having a radius a_o. Inside this sphere the dielectric constant is assumed to be unity, and outside the dielectric constant is the macroscopic value for the surrounding media. To represent the molecule as being on the surface of the embryo assume the x-y plane to be the interface between two media of different dielectric constants so that for $z > 0$, $\varepsilon = \varepsilon_1$ and for $z < 0$, $\varepsilon = \varepsilon_2$.

The electrostatic potential, Ψ, is most easily described in terms of spherical coordinates r, θ, ϕ. For $r > 0$, Ψ must satisfy Laplace's equation $\nabla^2\Psi(r,\theta,\phi) = 0$, the standard boundary conditions at $r = a_o$ and $r = \infty$, and at $r = 0$ have the singularities characteristic of the point dipole-quadrupole sources used to represent the fixed water molecule. The potential inside and outside the sphere of exclusion are assumed to have the form

$$\Psi_{in}(r,\theta,\phi) = \sum_{\ell=0}^{\infty}\sum_{m=-\ell}^{\ell}\left[A_{\ell m}r^{\ell} + B_{\ell m}r^{-(\ell+1)}\right]Y_{\ell m}(\theta,\phi)$$

$$\Psi_{out}(r,\theta,\phi) = \sum_{\ell=0}^{\infty}\sum_{m=-\ell}^{\ell} C_{\ell m}r^{-(\ell+1)}Y_{\ell m}(\theta,\phi), \qquad (4)$$

where $Y_{\ell m}(\theta,\phi) = P_{\ell}^{|m|}(\cos\theta)\exp(im\phi)$ are the unnormalized spherical harmonics which satisfy $\nabla^2 Y_{\ell m} + \ell(\ell+1)Y_{\ell m} = 0$. Requiring continuity of the potential and electric displacement at $r = a_o$ yields

$$A_{\ell m} = \left[\frac{(\ell+1)(1-\varepsilon)}{a_o^{2\ell+1}\{\ell+(\ell+1)\varepsilon\}}\right]B_{\ell m}$$
$$C_{\ell m} = \left[\frac{2\ell+1}{\ell+(\ell+1)\varepsilon}\right]B_{\ell m} \quad . \tag{5}$$

The final condition that ψ_{in} have the same singularities as a point dipole-quadrupole source given by

$$\psi(\bar{r}) = \frac{\bar{p}\cdot\bar{r}}{r^3} + \sum Q_{ij}(x_i x_j - \frac{1}{3}r^2\delta_{ij})\frac{1}{r^5} \tag{6}$$

where

$$\bar{p} = \int_v \rho(\bar{r})\bar{r}dv$$
$$Q_{ij} = \int_v \rho(\bar{r})(3x_i x_j - r^2\delta_{ij})dv \tag{7}$$

is used to evaluate the coefficients, $B_{\ell m}$.

Performing a term by term comparison of equations (4) and (6) expressed in spherical coordinates and using the explicit forms of the $y_{\ell m}(\theta,\phi)$ yields

$$B_{1,0} = p_z = p$$
$$B_{2,0} = Q_{zz} \tag{8}$$
$$B_{2,1} = B_{2,-1} = \frac{1}{12}(Q_{yy} - Q_{xx})$$

with all other $B_{\ell m}$'s vanishing.

The electrostatic field energy outside the sphere of exclusion is obtained by integrating the expression $W = \frac{1}{8\pi}\int_v \bar{D}\cdot\bar{E}\,dv$ over all space outside the sphere of exclusion. The integration must be performed in two parts: the first for $a_o \leq r \leq \infty$, $0 \leq \phi \leq 2\pi$ and $0 \leq \theta \leq \frac{\pi}{2}$ with $\bar{E} = -\nabla\psi_{out}(\varepsilon_1)$ and $\bar{D} = \varepsilon_1\bar{E}$; and the second for $a_o \leq r \leq \infty$, $0 \leq \phi \leq 2\pi$ and $\frac{\pi}{2} \leq \theta \leq \pi$ with $\bar{E} = -\nabla\psi_{out}(\varepsilon_2)$ and $\bar{D} = \varepsilon_2\bar{E}$. The sum of the two integrations yields

$$W = \frac{3p^2}{a_o^3}\left[\frac{\varepsilon_1}{(1+2\varepsilon_1)^2} + \frac{\varepsilon_2}{(1+2\varepsilon_2)^2}\right]$$
$$+ \frac{75pQ_{zz}}{32a_o^4}\left[\frac{\varepsilon_1}{(1+2\varepsilon_1)(2+3\varepsilon_1)} - \frac{\varepsilon_2}{(1+2\varepsilon_2)(2+3\varepsilon_2)}\right] \qquad (9)$$
$$+ \frac{1}{12a_o^5}\left[139Q_{zz}^2 - \frac{1}{4}(Q_{yy} - Q_{xx})^2\right]\left[\frac{\varepsilon_1}{(2+3\varepsilon_1)^2} + \frac{\varepsilon_2}{(2+3\varepsilon_2)^2}\right]$$

Based on the work of Weyl[29] and Fletcher,[30] the "normal" configuration of the surface is assumed to be with the dipoles directed into the liquid, therefore $\varepsilon_1 = \varepsilon_e$ and ε_2 = unity, and this energy is part of the macroscopic surface free energy which has already been accounted for in Eq. (1). However, if ε_1 = unity and $\varepsilon_2 = \varepsilon_e$, representing the dipole as directed out of the liquid, there is a difference in energy equivalent to twice the second term in Eq. (9) with $\varepsilon_1 = 1$ and $\varepsilon_2 = \varepsilon_e$,

$$\Delta W = \frac{75}{16}\frac{pQ_{zz}}{a_o^4}\left[\frac{1}{15} - \frac{\varepsilon_e}{(1+2\varepsilon_e)(2+3\varepsilon_e)}\right] \qquad (10)$$

At this point it is assumed that Eq. (10), which was derived for a plane interface, can be used to represent the energy difference between the two dipole orientations of a molecule on the curved surface of the embryo. Justification of the assumption is two fold: first, the liquid drop theory itself is at best a first approximation due to the use of macroscopic parameters, and second, the short range nature of both the dipole and quadrupole fields makes their region of influence very localized. It should be stressed, however, that applying Eq. (10) to a molecule in the curved surface of an embryo constitutes only a first approximation and is by no means exact.

The total difference in energy for an embryo with the surface dipoles directed out of the liquid compared to an embryo with the sur-

face dipoles directed into the liquid is given by $\Delta\Phi_{D-Q} = \Delta W g_s$, where g_s is the number of surface molecules. For an embryo of radius r, the number of surface molecules can be approximated by $g_s = 4\pi r^2/\pi a_o^2 = 4r^2/a_o^2$, where a_o is the effective radius of a surface molecule. This gives the difference in energy as

$$\Delta\Phi_{D-Q} = \frac{75pQ_{zz}}{4a_o^6}\left[\frac{1}{15} - \frac{\varepsilon_e}{(1+2\varepsilon_e)(2+3\varepsilon_e)}\right]r^2 \qquad (11)$$

for a cluster of radius r.

E. Dipole-Dipole Surface Correction Term

Abraham[31] has pointed out that a dipole-dipole interaction results when a small embryo is assumed to have an oriented dipole surface layer. The dipole-dipole interaction energy for a surface of parallel dipoles is included as part of the macroscopic surface free energy; however for a small embryo the radius of curvature has decreased to the point where, when oriented normal to the surface, two adjacent dipoles are no longer parallel and the interaction energy is increased. The curvature of the surface causes two adjacent dipoles each to be rotated through an angle $\xi/2$ with respect to the bisector of the line joining them. The angle ξ is directly related to the radius of the embryo by $\sin \xi/2 = a/2r$, where a is the separation distance of the dipoles (oxygen-oxygen distance). The deviation from parallel alignment increases the potential energy of a surface molecule by $\frac{1}{2}p^2(1-\cos\xi)n/a^3$, and the total increase for the surface is

$$\Delta\Phi_{D-D} = \tfrac{1}{2}[p^2(1-\cos\xi)ng_s/2a^3]. \qquad (12)$$

Here p is the permanent dipole moment, n, the number of nearest surface neighbors and g_s, the number of surface molecules. The prefactor of 1/2 is due to assigning half of the energy from each dipole-dipole

interaction to each of the two molecules taking part in the interaction.

The surface area on a sphere of radius, r, occupied by a molecule of diameter, a, is given by $\int_0^{\xi/2} 2\pi r^2 \sin\theta d\theta = 2\pi r^2(1-\cos\frac{\xi}{2})$, where $a/2 = r \sin\frac{\xi}{2}$. The number of surface molecules can then be approximated by the ratio of the total surface area to the surface area per molecule, or

$$g_s = \frac{4\pi r^2}{2\pi r^2(1-\cos\frac{\xi}{2})} = \frac{2}{(1-\cos\frac{\xi}{2})} . \tag{13}$$

Using Eq. (13) in Eq. (12) and assuming that ξ is small enough so that $1-\cos\xi \simeq \frac{\xi^2}{2}$, the total increase in dipole-dipole interaction energy for the surface reduces to

$$\Delta\Phi_{D-D} = \frac{p^2 n}{2a^3}\left(\frac{1-\cos\xi}{1-\cos\frac{\xi}{2}}\right) \simeq \frac{2p^2 n}{a^3} . \tag{14}$$

According to Fletcher's[30] model for the surface of water, the degree of orientation decays exponentially below the surface; therefore, the effective dipole moment per molecule in the m^{th} layer below the surface is $2p(\alpha_m - \frac{1}{2})$, where $\alpha_m = \frac{1}{2}+(\alpha_o-\frac{1}{2})e^{-\gamma m}+\cdots$ with α being the orientation parameter and γ the orientation decay parameter. The total dipole-dipole interaction energy for the embryo is obtained by substituting the effective dipole moment into Eq. (14) and integrating over the number of molecular layers giving

$$\Delta\Phi_{D-D} = \frac{2np^2}{a^3}\int_0^{m_r} 4(\alpha_m-\tfrac{1}{2})^2 dm = \frac{4np^2}{a^3\gamma}(\alpha_o-\tfrac{1}{2})^2(1-e^{-\gamma m_r}) . \tag{15}$$

For an embryo of radius r, it is assumed that there are $m_r = \frac{r}{a}$ molecular layers.

At this point note is taken of the fact that water molecules interact by hydrogen bonding, and this prevents the dipoles from being

oriented normal to the surface. Therefore the effective dipole moment per molecule is p cos θ_o, where θ_o is the angle the dipoles make with the surface normal, and Eq. (15) becomes

$$\Delta\Phi_{D\text{-}D} = \frac{4np^2\cos^2\theta_o}{\gamma a^3}(\alpha_o-\tfrac{1}{2})^2(1-e^{-\gamma r/a}). \tag{16}$$

F. Total Corrected Change in Free Energy

The total change in free energy for an embryo nucleating on an ion is given by summing Eq. (1), (3), (11) and (16).

$$\begin{aligned}\Delta\Phi_T(g) = &-(\phi_A-\phi_B)g + 4\pi\sigma_o\mu^{2/3}g^{2/3} - \frac{e^2}{2}\left(1-\frac{1}{\varepsilon_e}\right)\left(\frac{1}{r_e}-\frac{1}{\mu^{1/3}g^{1/3}}\right)\\ &+\frac{75pQ_{zz}}{4a_o^6}\left[\frac{1}{15}-\frac{\varepsilon_e}{(1+2\varepsilon_e)(2+3\varepsilon_e)}\right]\mu^{2/3}g^{2/3}\left(\frac{1+\delta}{2}\right)\\ &+\frac{4np^2\cos^2\theta_o}{\gamma a^3}(\alpha_o-\tfrac{1}{2})^2\left[1-e^{-\frac{\gamma\mu^{1/3}g^{1/3}}{a}}\right],\end{aligned} \tag{17}$$

where δ has the same sign as the ionic charge and a magnitude of unity. The conversion from the radius, r, to the number of molecules in the embryo, g, is made using the relationship $r^3 = \mu g$. This assumes the standard liquid drop approximation that $\frac{4}{3}\pi r^3 = v_B g$, where v_B is the molecular volume in the liquid state.

G. Embryos in Stable and Unstable Equilibrium

For homogeneous nucleation Eq. (1) exhibits a maximum for an embryo of g_* molecules, which represents an embryo that is in unstable equilibrium with the surrounding vapor. The embryo of size g_* is referred to as a critical nucleus because once the embryo becomes larger than g_* it is free growing and can grow to macroscopic size with a continuous decrease in free energy.

The change in free energy for nucleation on ions, Eq. (17),

exhibits not only a maximum at $g = g_*$, but also a minimum for $g = g_o$, $(g_* > g_o)$, representing a small stable embryo which forms about the ion by hydration, see Figure 4.

The values of g_o and g_* can be determined by setting $\frac{\partial(\Delta\Phi_T)}{\partial g}$ equal to zero.

$$\frac{\partial(\Delta\Phi_T)}{\partial g} = 0 = -(\phi_A-\phi_B) + \frac{8\pi\sigma_o\mu^{2/3}}{3} g^{-1/3} - \frac{e^2}{6}(1-\frac{1}{\varepsilon_e})\mu^{-1/3}g^{-4/3}$$

$$+ \frac{25pQ_{zz}}{2a_o^6}\left[\frac{1}{15} - \frac{\varepsilon_e}{(1+2\varepsilon_e)(2+3\varepsilon_e)}\right]\mu^{2/3}g^{-1/3}\left[\frac{1+\delta}{2}\right] \qquad (18)$$

$$+ \frac{4np^2\cos^2\theta_o\gamma}{3a^4}\left[\frac{(\alpha_o-\frac{1}{2})^2}{\gamma}\right] e^{\frac{-\gamma\mu^{1/3}g^{1/3}}{a}} \mu^{1/3}g^{-2/3} .$$

Differentiating Eq. (18) at constant temperature and assuming that the relations $d\phi_A = -v_A dp$ and $d\phi_B = -v_B dp$ are valid (v_A = molecular volume in the gas phase), then

$$(v_A - v_B)dp = d\{\frac{8\pi\sigma_o\mu^{2/3}}{3} g^{-1/3} - \frac{e^2}{6}(1-\frac{1}{\varepsilon_e})\mu^{-1/3}g^{-4/3}$$

$$+ \frac{25pQ_{zz}}{2a_o^6}\left[\frac{1}{15} - \frac{\varepsilon_e}{(1+2\varepsilon_e)(2+3\varepsilon_e)}\right]\mu^{2/3}g^{-1/3}\left[\frac{1+\delta}{2}\right] \qquad (19)$$

$$+ \frac{4np^2\cos^2\theta_o\gamma}{3a^4}\left[\frac{(\alpha_o-\frac{1}{2})^2}{\gamma}\right] e^{\frac{-\gamma\mu^{1/3}g^{1/3}}{a}} \mu^{1/3}g^{-2/3}\} .$$

If v_B is neglected compared to v_A and the vapor is treated as an ideal gas, so that $v_A = kT/p$, then Eq. (19) becomes

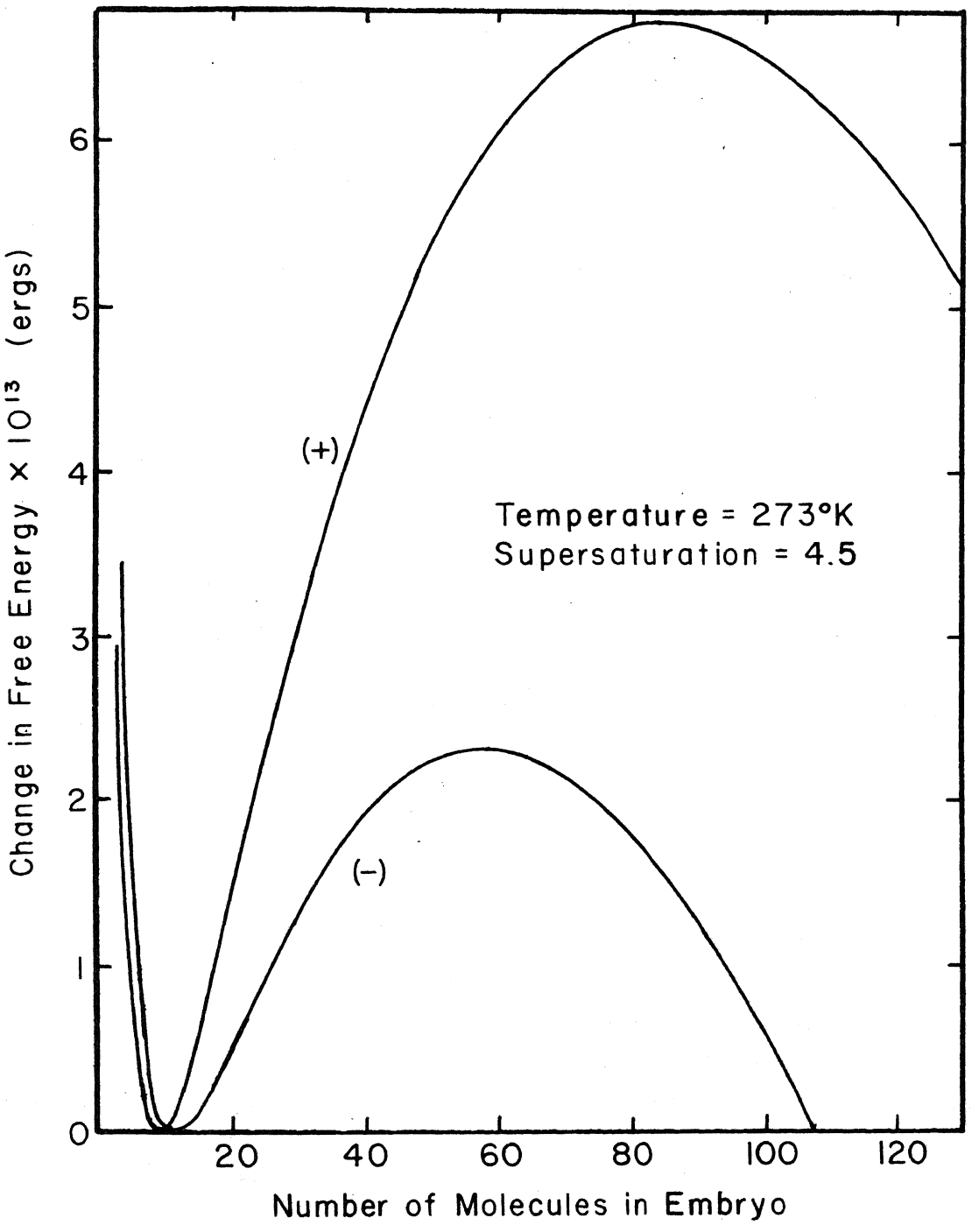

Figure 4. Change in free energy as a function of embryo size.

$$kT\, d(\ln P) = d\left\{\frac{8\pi\sigma_o\mu^{2/3}}{3}g^{-1/3} - \frac{e^2}{6}\left(1-\frac{1}{\varepsilon_e}\right)\mu^{-1/3}g^{-4/3}\right.$$

$$+\frac{25pQ_{zz}}{2a_o^6}\left(\frac{1}{15}-\frac{\varepsilon_e}{(1+2\varepsilon_e)(2+3\varepsilon_e)}\right)\mu^{2/3}g^{-1/3}\left(\frac{1+\delta}{2}\right) \qquad (20)$$

$$\left.+\frac{4np^2\cos^2\theta_o\gamma}{3a^4}\left(\frac{(\alpha_o-\frac{1}{2})^2}{\gamma}\right)e^{\frac{-\gamma\mu^{1/3}g^{1/3}}{a}}\mu^{1/3}g^{-2/3}\right\} .$$

As $g \to \infty$, $p \to p_\infty$, where p_∞ is the macroscopic vapor pressure of the liquid at temperature T. Integrating Eq. (20) from p_∞ to p and from ∞ to g yields

$$kT\, \ln\left(\frac{p}{p_\infty}\right) = \frac{8\pi\sigma_o\mu^{2/3}}{3}g^{-1/3} - \frac{e^2}{6}\left(1-\frac{1}{\varepsilon_e}\right)\mu^{-1/3}g^{-4/3}$$

$$+\frac{25pQ_{zz}}{2a_o^6}\left(\frac{1}{15}-\frac{\varepsilon_e}{(1+2\varepsilon_e)(2+3\varepsilon_e)}\right)\mu^{2/3}g^{-1/3}\left(\frac{1+\delta}{2}\right) \qquad (21)$$

$$+\frac{4np^2\cos^2\theta_o\gamma}{3a^4}\left(\frac{(\alpha_o-\frac{1}{2})^2}{\gamma}\right)e^{\frac{-\gamma\mu^{1/3}g^{1/3}}{a}}\mu^{1/3}g^{-2/3} .$$

Eq. (21) is the Kelvin-Thomson relation from the homogeneous nucleation theory modified to account for the effects of the ion. In the homogeneous theory the relation has one root for a given value of $S = \frac{p}{p_\infty}$ (S = supersaturation ratio) representing the size of the critical nucleus (g_*), while Eq. (21) has two roots g_o and g_* ($g_* > g_o$) corresponding to the small stable hydration embryo and the critical nucleus respectively, see Figure 5.

H. Nucleation Kinetics

The formulation of the nucleation kinetics presented in this section follows very closely the homogeneous nucleation kinetics as presented by Frenkel.[5] For any condition of the vapor (either sub-

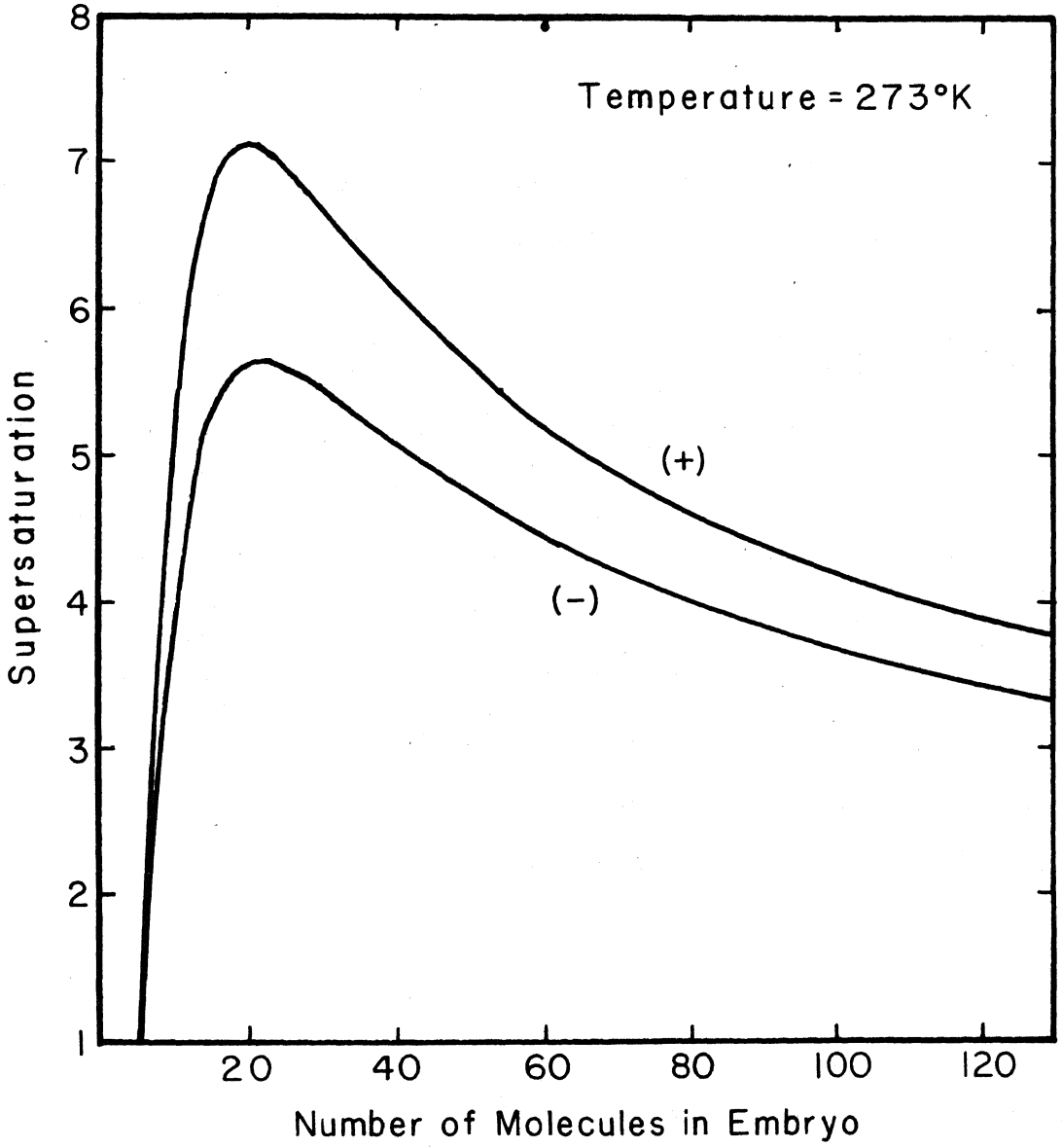

Figure 5. Modified Kelvin-Thomson relation.

saturated or supersaturated) there will exist a distribution in the size of embryos surrounding the ions, due to local fluctuations in free energy, given by Boltzmann's formula

$$N_g = N_o \exp - (\Delta\Phi_g - \Delta\Phi_{g_o})/kT, \tag{22}$$

where $\Delta\Phi_g$ and $\Delta\Phi_{g_o}$ are given by Eq. (17), N_o, the hydrated ion density, (the hydration embryo is assumed to contain g_o molecules), and N_g, the density of embryos of size g. For a subsaturated vapor N_g decreases continuously as g increases, but for a supersaturated vapor N_g passes through a minimum at $g = g_*$ and then increases to infinity as g goes to infinity. The latter situation is obviously not true since it predicts the physically impossible condition of an infinite number of infinitely large drops. The standard solution to the dilemma presented by Eq. (22) is to assume that when a supersaturated condition is established the system does not attain the equilibrium distribution predicted by Eq. (22), but instead rapidly achieves a steady state distribution such that $N_G = 0$, for some $G >> g_*$. In the steady state condition the distribution is constant with respect to time; however there is a net flux of embryos passing through the distribution. To maintain a constant vapor density it is assumed that as the embryos reach a size g = G they are removed from the system, counted as drops and their molecules returned to the vapor as monomers.

The growth of the embryos is assumed to proceed by the acquisition and loss of single vapor molecules; the process can be represented by a set of reaction formulas:

$$\begin{aligned}
A_{g_o} + A_1 &\leftrightharpoons A_{g_o+1} \\
A_{g_o+1} + A_1 &\leftrightharpoons A_{g_o+2} \\
&\vdots \\
A_g + A_1 &\leftrightharpoons A_{g+1} \\
&\vdots \\
A_{G-1} + A_1 &\rightarrow A_G ,
\end{aligned} \tag{23}$$

where A_g and A_1 are an embryo of g molecules and a monomer respectively. The reaction formulas yield a set of time dependent concentration equations

$$\frac{\partial}{\partial t}n_{g_o} = -\lambda_{g_o} n_{g_o} + \lambda'_{g_o+1} n_{g_o+1}$$

$$\begin{aligned}
\frac{\partial}{\partial t}n_{g_o+1} &= \lambda_{g_o} n_{g_o} - (\lambda_{g_o} + \lambda'_{g_o+1}) n_{g_o+1} + \lambda'_{g_o+2} n_{g_o+2} \\
&\vdots \qquad\qquad\qquad \vdots \\
\frac{\partial}{\partial t}n_g &= \lambda_{g-1} n_{g-1} - (\lambda_g + \lambda'_g) n_g + \lambda'_{g+1} n_{g+1} \\
&\vdots \qquad\qquad\qquad \vdots \\
\frac{\partial}{\partial t}n_{G-1} &= \lambda_{G-2} n_{G-2} - (\lambda_{G-1} + \lambda'_{G-1}) n_{G-1} .
\end{aligned} \tag{24}$$

n_g is the nonequilibrium time dependent density of embryos of size g, λ_g, the rate at which embryos grow from size g to g+1 and λ'_g, the rate at which embryos decay from size g to g-1. Under the assumption of steady state $\frac{\partial}{\partial t}n_g = 0$ for all g and the flux of embryos passing through the distribution at size g is

$$J_g = \lambda_{g-1} n_{g-1} - \lambda'_g n_g . \tag{25}$$

The reaction rates λ_g and λ'_g can be expressed in terms of the embryo surface area and the rate per unit area of condensation and evaporation of molecules.

$$\begin{aligned}
\lambda_g &= 4\pi\mu^{2/3} g^{2/3} \beta \\
\lambda' g &= 4\pi\mu^{2/3} g^{2/3} \beta'
\end{aligned} \tag{26}$$

with β and β' (assumed independent of g) as the condensation and evaporation rates per unit area for an embryo. The principle of detailed balance requires that $N_g \lambda'_g = N_{g-1} \lambda_{g-1}$, and for equilibrium at $g = g_*$, $\lambda_{g_*} = \lambda'_{g_*}$.

Eq. (25) can now be written as

$$J_g = \lambda_{g-1} N_{g-1} \left(\frac{n_{g-1}}{N_{g-1}} - \frac{n_g}{N_g} \right) \tag{27}$$

leading to

$$\frac{\partial n_g}{\partial t} \simeq J_g - J_{g+1} \, , \tag{28}$$

which is the equation which must be evaluated. Except for very small values of g, the quantities in Eq. (25) change very slightly for $\Delta g = \pm 1$. On this basis it is assumed that n_g can be treated as a continuous function of g, n(g), and if $\lambda_{g-1} \simeq \lambda_g = \lambda(g)$ then

$$J(g) = -N(g)\lambda(g) \frac{\partial}{\partial g} \left[\frac{n(g)}{N(g)} \right] \tag{29}$$

or

$$J = -\lambda \frac{\partial n}{\partial g} + \lambda n \frac{\partial}{\partial g} \ln N \, . \tag{30}$$

Since $N(g) = N_o \exp - [(\Delta\Phi_g - \Delta\Phi_{g_o})/kT]$

$$J = -\lambda \frac{\partial n}{\partial g} - \frac{\lambda}{kT} \frac{\partial}{\partial g} (\Delta\Phi_g - \Delta\Phi_{g_o}) \, , \tag{31}$$

where $\Delta\Phi_g$ and $\Delta\Phi_{g_o}$ are given by Eq. (17).

Replacing $J_g - J_{g+1}$ by $-\frac{\partial J}{\partial g}$ in Eq. (28) and then using Eq. (31) for J gives

$$\frac{\partial n}{\partial t} = \frac{\partial}{\partial g} \left(\lambda \frac{\partial n}{\partial g} \right) + \frac{1}{kT} \frac{\partial}{\partial g} \left(\lambda n \frac{\partial [\Delta\Phi_g - \Delta\Phi_{g_o}]}{\partial g} \right) \, . \tag{32}$$

Assuming that the time required to establish a steady state can be neglected,[10] then J is a constant and n(g) can be found from Eq. (29) by a simple integration

$$n(g) = JN(g) \int_g^G \frac{dg}{\lambda(g) N(g)} \tag{33}$$

using the boundary condition that n(G) = 0.

Again using $N(g) = N_o \exp - [(\Delta\Phi_g - \Delta\Phi_{g_o})/kT]$, $\Delta\Phi_g$ and $\Delta\Phi_{g_o}$ from Eq. (17), Eq. (33) becomes

$$n(g) = J\{\exp - [(\Delta\Phi_g - \Delta\Phi_{g_o})/kT]\}\int_g^G \frac{1}{\lambda(g)} \exp [(\Delta\Phi_g - \Delta\Phi_{g_o})/kT]dg \qquad (34)$$

for values near $g = g_*$.

Since $\exp [(\Delta\Phi_g - \Delta\Phi_{g_o})/kT]$ has a sharp maximum at $g = g_*$ and $\lambda(g)$ has only a weak dependence on g compared to $\exp [(\Delta\Phi_g - \Delta\Phi_{g_o})/kT]$, $\lambda(g)$ can be replaced by $\lambda(g_*) = \lambda_*$ and $(\Delta\Phi_g - \Delta\Phi_{g_o})$ expanded about $g = g_*$ neglecting terms higher than second order.

$$(\Delta\Phi_g - \Delta\Phi_{g_o}) = (\Delta\Phi_{g_*} - \Delta\Phi_g) + \left(\frac{\partial^2\Delta\Phi_g}{\partial g^2}\right)_{g=g_*} \frac{(g-g_*)^2}{2} . \qquad (35)$$

Substituting Eq. (35) into Eq. (34) for $(\Delta\Phi_g - \Delta\Phi_{g_o})$ yields

$$n(g) = \frac{J}{\lambda_*}\{\exp [(\Delta\Phi_{g_*} - \Delta\Phi_g)/kT]\}\int_{-(g_*-g)}^{G-g_*} \exp [(\frac{\partial^2\Delta\Phi_g}{\partial g^2})_{g=g_*} \frac{(g-g_*)^2}{2kT}]d(g-g_*). \qquad (36)$$

The quantity $[kT/-\frac{\partial^2\Delta\Phi}{\partial g^2}]^{1/2}_{g=g_*}$ is a measure of the width of the maximum of the function $1/N(g)$ near g_*, and if both (g_*-g) and $(G-g_*)$ are large compared to $[kT/-\frac{\partial^2\Delta\Phi}{\partial g^2}]^{1/2}_{g=g_*}$ then the limits of integration can be replaced by $\pm\infty$ and Eq. (36) integrated in closed form. If $\exp - [(\Delta\Phi_g - \Delta\Phi_{g_o})/kT]$ is replaced by $N(g)/N_o$ the result is

$$\frac{n(g)}{N(g)} = \frac{J}{N_o\lambda_*} \exp [(\Delta\Phi_{g_*} - \Delta\Phi_{g_o})/kT]\left(\frac{2\pi kT}{-\frac{\partial^2\Delta\Phi}{\partial g^2}}\right)^{\frac{1}{2}}_{g=g_*} = \text{Constant} \qquad (37)$$

for $g < g_* - [kT/-\frac{\partial^2\Delta\Phi}{\partial g^2}]^{1/2}_{g=g_*}$.

In the range $1 \leq g \lesssim g_* - [kT/-\frac{\partial^2\Delta\Phi}{\partial g^2}]^{1/2}_{g=g_*}$ the ratio $n(g)/N(g)$ is nearly unity and then above this range falls rapidly to zero. Setting the constant in Eq. (37) equal to one yields

$$J = N_o\lambda_*[-\frac{\partial^2\Delta\Phi}{\partial g^2}/2\pi kT]^{\frac{1}{2}}_{g=g_*} \exp - [(\Delta\Phi_{g_*} - \Delta\Phi_{g_o})/kT] . \qquad (38)$$

From Eq. (26) $\lambda_* = 4\pi\mu^{2/3}g_*^{2/3}\beta$ and from kinetic considerations $\beta = C_o p/(2\pi mkT)^{1/2}$, where p is the vapor pressure, m, the mass of a

vapor molecule and C_o, the accomodation coefficient.

I. Limitations of the Theory

As the supersaturation of the system increases $g_o \rightarrow g_*$ and the potential barrier hindering growth of the embryos becomes progressively lower until it vanishes when $g_o = g_*$. The theory loses its validity as $g_o \rightarrow g_*$ due to the failure of the approximation used to integrate Eq. (33). Since $[\Delta\Phi(g_*) - \Delta\Phi(g_o)] \rightarrow 0$ as $g_o \rightarrow g_*$, the exponential can no longer be considered to have a sharp maximum at g_*, which permitted the use of a power series expansion and extension of the integration limits to $\pm\infty$.

Based on the present theory, as the supersaturation exceeds the value for which $g_o = g_*$, there is no longer a potential barrier for nucleation and the ions nucleate instantaneously. From a physical standpoint the nucleation cannot be instantaneous but will be governed by the kinetics of supplying vapor molecules to the growing embryos. From an experimental point of view, the nucleation rate becomes so large that all the ions would have nucleated in less time than would be required to establish a supersaturation large enough to invalidate the theory. It should be noted that the limitation is due to the kinetic portion of the treatment and not the thermodynamic portion.

IV. RESULTS AND DISCUSSION

The general agreement between experimental and theoretical results, as shown in Figure 6, is very good. The experimental data has been normalized to an initial ion density of 35 ions per cc. The supersaturation plotted is the peak supersaturation attained by the chamber, using the pulsed operation shown in Figure 2B. The three experimental curves represent the results of positive ions in argon, negative ions in argon and negative ions in helium. The theoretical curves were obtained by numerically integrating the nucleation rate, Eq. (38), over a parabolic supersaturation pulse which closely approximates the chamber expansion pulse. The depletion of ions due to nucleation was taken into account. The total number of drops "nucleated" was plotted against the peak supersaturation.

Not only do the magnitudes and slopes of the experimental and theoretical results agree very well, but the difference in slope between the experimental curves for positive and negative ions is matched by a similar difference in the slopes of the theoretical curves. The absence of experimental data for positive ions in helium reflects the confirmation of earlier work done in this laboratory which indicated that positive helium ions will not catalize the nucleation process. It is believed that this is due to some mechanism which prevents the formation of the initial hydration cluster about the positive helium ions.

The values of the parameters and physical constants used to calculate the theoretical curves, shown in Figure 6, are listed in Table I. The value of $\varepsilon_e=3.4$ used to obtain agreement with the experimental results is very close to the high frequency dielectric constant of ice,

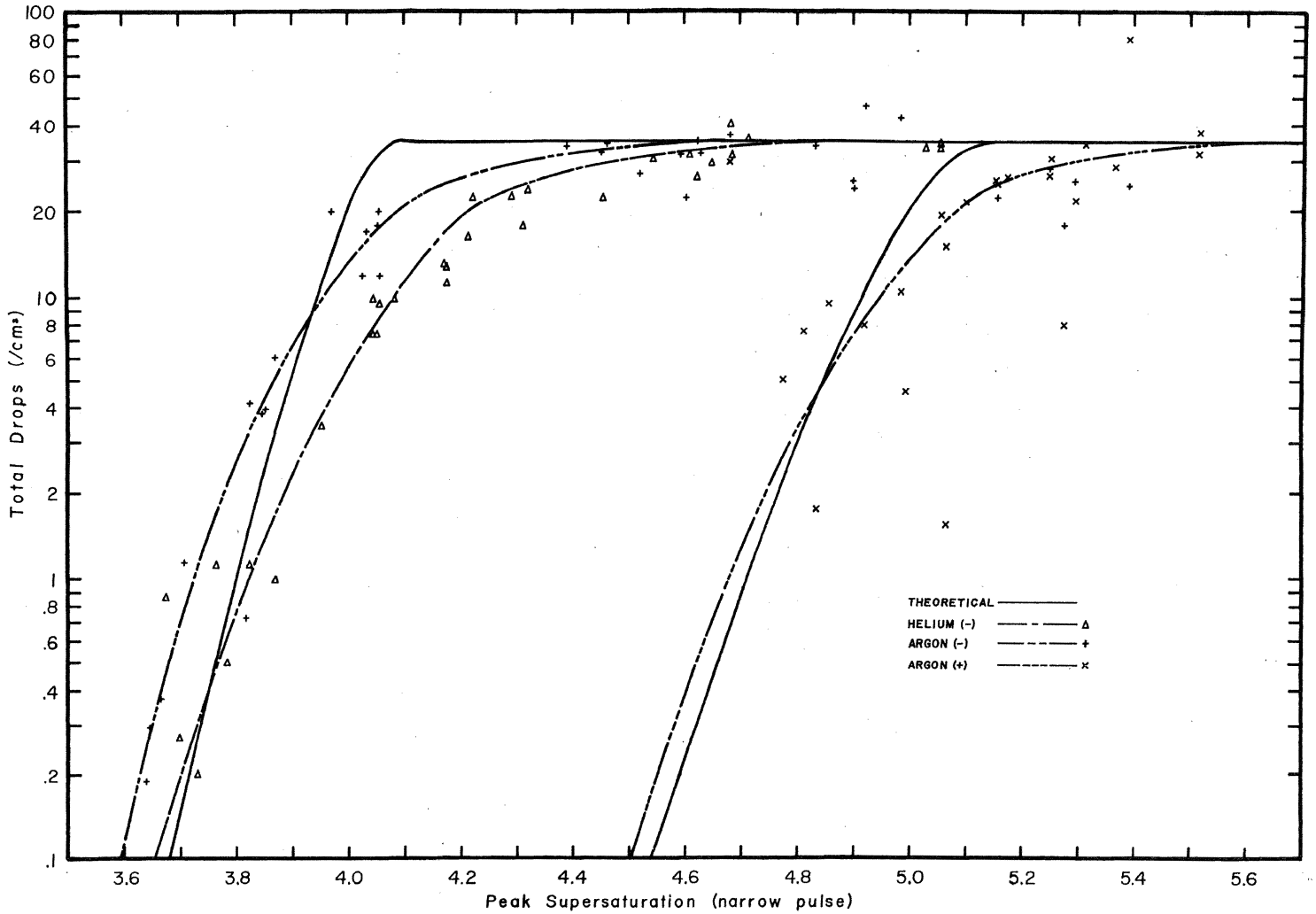

Figure 6. Number of droplets nucleated as a function of peak supersaturation. Initial Temperature = 25.0°C.

TABLE I

Values of Parameters and Physical Constants

Used in the Theoretical Calculations

$e = 4.8 \times 10^{-10}$ esu

$p = 1.87 \times 10^{-18}$ esu-cm

$Q_{zz} = .364 \times 10^{-26}$ esu-cm^2

$k = 1.38 \times 10^{-16}$ erg/°K

$\sigma_o = (116.459 - .149228 \times T)$ erg/cm^2 (T in °C)

$a = 2.76 \times 10^{-8}$ cm

$\Theta_o = 55°$

$\gamma = .074$

$\frac{(\alpha_o - \frac{1}{2})^2}{\gamma} = 3.4$

$n = 3$

$\mu = 7.1382 \times 10^{-24}$ cm^3

$a_o = 1.86 \times 10^{-8}$ cm

$\varepsilon_e = 3.4$

$C_o = 0.56$

3.2,[32] indicating the molecules are tightly bound, preventing any contribution to the dielectric constant by rotational orientation of the permanent molecular dipole moment.

The separation of the theoretical curves for positive and negative ions is extremely sensitive to the radius of the sphere of exclusion, a_o, used in the derivation of the dipole-quadrupole term. The value of 1.86×10^{-8} cm is in good agreement with other estimates of the molecular radius which range from 1.38×10^{-8} cm, oxygen-oxygen separation distance in ice, to 3.1×10^{-8} cm, volume per molecule in bulk liquid. The latter is expected to be too large since it includes the free volume as well as the central hard core of the molecule.

The value for the permanent quadrupole moment can vary depending on the source of the measurement. All of the values normally listed are of the same order of magnitude, and the variations can be offset by very small adjustments in the value used for a_o, the radius of the sphere of exclusion, which is only an estimate at best.

The nucleation rate, as given in Eq. (38), is directly proportional to the ion density, which in practice can not be treated as a constant. However, if the nucleation rate, J, is considered as the fractional rate of decay of ions into droplets, then

$$-dN = Jdt = N\Gamma dt \ , \tag{39}$$

where N is the number of ions present. Integrating from N_o to N and 0 to t

$$N = N_o e^{-\Gamma t}, \tag{40}$$

where N is the number of ions which have not been nucleated upon after time t. $\Gamma = J/N_o$ has the form of a decay constant or alternatively may be interpreted as the probability per unit time that an ion will serve as a center for nucleation. The fraction of ions which have served as centers for nucleation after time t is just $1-e^{-\Gamma t}$; or the den-

sity of drops, N_d, is given by

$$N_d = N_o(1-e^{-\Gamma t}), \tag{41}$$

where N_o is the initial ion density.

An examination of previous work, as listed by Mason[1] and shown in Table II, shows that the "critical supersaturation" listed are consistently higher than the results of the present work. If nucleation on 10% of the ions present is used as the criterion for a "critical supersaturation", then for negative ions the present work yields a "critical supersaturation" of 3.83 in argon and 3.9 in helium. The range of 4.1 to 4.2 listed in literature corresponds to nucleation on 50-75% of the ions in argon and 30-50% of the ions in helium for the present work.

A closer examination of the work listed in the literature reveals several factors which would cause previous work to yield higher supersaturations than the present work. When the expansion of a cloud chamber causes the temperature of the vapor-gas mixture to decrease, the walls, which are still at the initial temperature, immediately begin heating the layer of gas next to them causing it to expand, partially recompressing the central region of the sensitive volume. Due to this partial recompression, the vapor-gas mixture never reaches the temperature and supersaturation which are predicted by theory for an adiabatic expansion between two fixed volumes. Therefore, the supersaturations calculated for volume expansion ratios by the workers listed in Table II are consistantly higher than the supersaturations actually achieved by their chambers. The small size of the chambers which they used enhanced the effect which is proportional to the surface to volume ratio of the chamber. The small size of the chambers also caused their natural sensitive times to be very short so that higher supersaturations were required to obtain drop densities which could be observed visually. Moreover, if the equilibrium ion density obtained in a chamber without a field is

TABLE II*

Review of Experimental Results as Compiled by Mason

	Ion Sign	T_1(°K)	T_2	(V_2/V_1)	S
Wilson[33]	-	293	267.8	1.252	4.2
	+	293	---	1.31	6.0
Przibram[34]	-	293	---	1.236	3.7
	+	293	---	1.31	6.0
Laby[35]	-	---	267.6	1.256	4.2
Andren[36]	-	---	267.8	1.253	4.1
Powell[37]	-	291	266.5	1.245	3.98
Flood[38]	-	---	265	1.252	4.1
Loeb, Kip and Einarsson[24]	-	295	---	1.25	---
	+	295	---	1.31	---
Scharrer[39]	-	292	---	1.25	4.14
	+	292	---	1.28	4.87
Sander and Damkkohler[40]	-	---	265	---	3.9

*This table is reporduced with minor changes from "The Physics of Clouds" by B. J. Mason, p. 22.

used, the diffusion of ions to the walls also depends upon the dimensions of the chamber and the surface to volume ratio. Therefore, small chambers arrive at a smaller equilibrium ion density, and a greater proportion of the ions would have to be nucleated upon to make the droplet density readily observable.

The experimental methods used in the present work have circumvented most of these problems. The use of a sensitive pressure transducer to measure the pressure in the sensitive volume automatically includes the compressive effects of the wall heating in the data used to calculate the temperature and supersaturation. The use of a much larger chamber has increased the natural sensitive time to the point where the effective sensitive time is controlled by a deliberate partial recompression of predetermined magnitude, see Figure 2B. The use of photography and a high intensity lighting system decreases the drop density required to determine the onset of nucleation and permits more accurate determination of the absolute magnitude of the densities. With these considerations in mind the agreement between the present experimental results and those obtained by earlier workers is not unreasonable.

The primary experimental uncertainty in the present work was the value of the local ion density. This uncertainty was due to the failure of the ions, which tended to be formed in clusters or short tracks by the action of individual Compton electrons, to diffuse into a uniform density. Increasing the time between the creation of the ions and the expansion of the chamber caused a decrease in both the ion density and the certainty with which the two signs of charge could be separated.

The dipole-dipole correction term to the change in free energy does not vanish if the ionic charge is set equal to zero, corresponding to

homogeneous nucleation. Since this term has not previously been included in the classical liquid drop treatment, a comparison was made with the experimental data of Allen and Kassner.[15] The comparison with their homogeneous nucleation measurements for an initial temperature of 22.5°C is shown in Figure 7. The theoretical fit was obtained using an accommodation coefficient of 0.56, which was then used in calculating the theoretical curves for both positive and negative ions shown in Figure 6. The fact that the theory is capable of predicting both the magnitude and slope of not only the nucleation on positive and negative ions but also homogeneous nucleation supports the assumptions made in attributing an oriented dipole surface layer to both the liquid water and the prenucleation embryos.

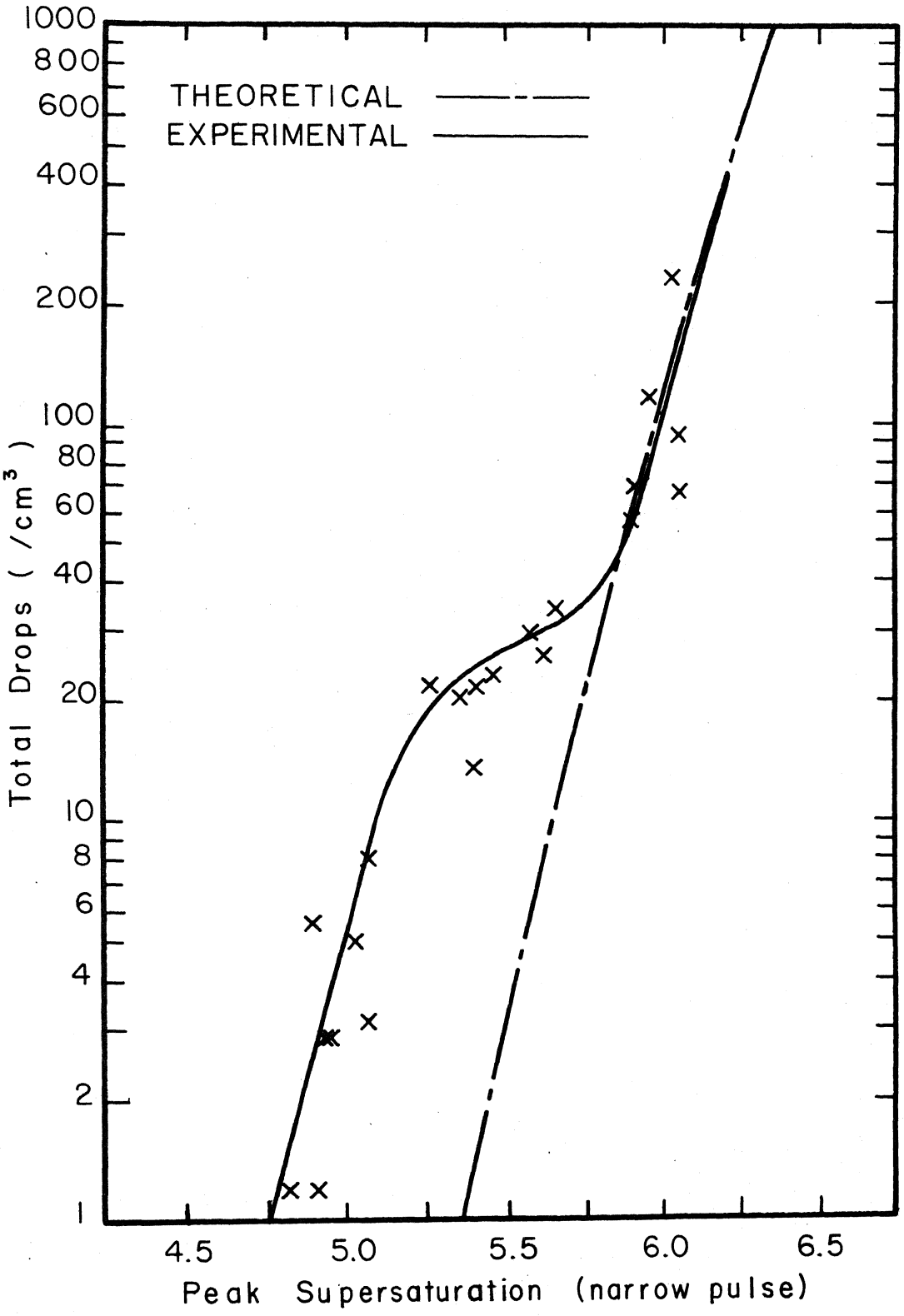

Figure 7. Comparison with homogeneous nucleation data of Allen and Kassner.[15] Initial Temperature 22.5°C.

V. CONCLUSIONS

The theoretical treatment developed in this work to describe the sign preference for nucleation on ions is based on the idea that the surface of liquid water has an oriented dipole surface layer and comprises an extension of the classical liquid drop treatment as presented by Frenkel.[5] The value of the effective dielectric constant required to achieve agreement between theoretical and experimental results is only slightly greater than the high frequency value observed for ice, indicating that the prenucleation embryos possess a rigid tightly bound structure. Moreover, the dipole-dipole correction to the free energy of the neutral embryos, which decreases the nucleation rate by a factor of approximately 10^3, provides agreement between the results of the classical theory and the "true" homogeneous nucleation measurements of Allen and Kassner[15] when an accommodation coefficient of 0.56 is used. The dipole-dipole correction results from the oriented dipole surface layer, a surface property peculiar to polar hydrogen-bonded substances, such as water, which has not previously been taken into account. Using a single set of values for the theoretical parameters, the present work achieves agreement between theoretical and experimental results for both homogeneous nucleation and nucleation on positive and negative ions.

When the heterogeneous component[15] is properly taken into account, the classical homogeneous nucleation rate, as given by Frenkel[5] (p. 396, Eq. 27b), predicts results about 10^3 greater than the experimentally obtained nucleation rates. The dipole-dipole correction brings the theoretical results into almost perfect agreement with experimental results. It is difficult to reconcile the so called "correction terms", which increase the nucleation rate by a factor of 10^{17}, advocated by Lothe and Pound[19] with these results.

VI. BIBLIOGRAPHY

1. B. J. Mason, "The Physics of Clouds" (Oxford University Press, New York, 1957).

2. M. Volmer and A. Weber, Z. Physik, Chem. A119, 277 (1926).

3. L. Farkas, Z. Physik, Chem. (Lepizig) A125, 236 (1926).

4. R. Becker and W. Doring, Ann. Physik. 24, 719 (1935).

5. J. Frenkel, J. Chem. Phys. 7, 538 (1939); "Kinetic Theory of Liquids" (Dover Publications Inc., New York, 1946), pp. 336-426.

6. J. Zeldovich, J. Exptl. Theoret. Phys. (U.S.S.R.) 12, 525 (1942).

7. T. Glosios, Kolloid Z. 80, 269 (1937).

8. N. N. Das Gupta and S. K. Ghosh, Rev. Mod. Phys. 18, 225 (1946).

9. G. Thomfor and M. Volmer, Ann. Physik. 33, 109 (1938).

10. D. Stachorska, J. Chem. Phys. 42, 1887 (1965).

11. K. C. Russell, J. Chem. Phys. 50, 1809 (1969).

12. J. L. Katz and B. J. Ostermier, J. Chem. Phys. 47, 478 (1967).

13. P. P. Wegener, J. Appl. Phys. 25, 1485 (1954).

14. P. P. Wegener and A. A. Pouring, Phys. Fluids 1, 352 (1964).

15. L. B. Allen and J. L. Kassner, Jr., J. Colloid and Interface Sci. 30, 81 (1969).

16. J. G. Smith. J. L. Kassner, Jr. and A. H. Biermann, J. Rech. Atmospherique 3, 41 (1968).

17. R. Dawborn, "A Study of Re-Evaporation Nuclei," M.S. Thesis, University of Missouri - Rolla (unpublished).

18. J. L. Kassner, Jr. and R. J. Schmitt, J. Chem. Phys. 44, 4166 (1966).

19. J. Lothe and G. M. Pound, J. Chem. Phys. 36, 2080 (1962).

20. H. Reiss and J. L. Katz, J. Chem. Phys. 46, 2496 (1967).

21. H. Reiss, J. L. Katz and E. R. Cohen, J. Chem. Phys. 48, 5553 (1968).

22. F. F. Abraham, Science 168, 833 (1970).

23. J. J. Thomson, "Conduction of Electricity Through Gasses" (Cambridge University Press), pp. 325-334.

24. L. B. Loeb, A. F. Kip and A. W. Einarsson, J. Chem. Phys. 6, 264 (1939).

25. R. J. Good, J. Phys. Chem. 61, 810 (1957).

26. F. F. Abraham, Appl. Phys. Letters 13, 208 (1968).

27. F. F. Abraham, J. Appl. Phys. 39, 5811 (1969).

28. F. H. Stillinger and A. Ben-Naim, J. Chem. Phys. 47, 4431 (1967).

29. W. A. Weyl, J. Coll. Sci. 6, 389 (1951).

30. N. H. Flecther, Philo. Mag. 7, 255 (1962).

31. F. F. Abraham, J. Chem. Phys. 50, 3977 (1969).

32. N. H. Fletcher, "The Chemical Physics of Ice" (Cambridge University Press), pp. 198-200.

33. C. T. R. Wilson, Phil. Trans. Roy. Soc. A189, p. 265 (1899).

34. K. Prizbram, Sitzungsber. Akad. Wiss. Wien 115, p. 33 (1906).

35. T. A. Laby, Phil. Trans. Roy. Soc. A208, p. 445 (1908).

36. L. Andren, Ann. Phys. (Lepizig) 52, p. 1 (1917).

37. C. F. Powell, Proc. Roy. Soc. A119, p. 553 (1928).

38. H. Flood, "Kinetik Der Phasenbildung" by M. Volmer, (Steinkopff, Dresden and Lepizig, 1939).

39. L. Scharrer, Ann. Der Phys. 35, p. 619 (1939).

40. A. Sander and G. Damkohler, Die Naturwiss. 31, p. 460 (1943).

VII. VITA

Daniel Ralph White was born on April 21, 1940, in Kansas City, Missouri. He received his primary and secondary education in the Kansas City, Missouri public schools, graduating in June 1958. He entered the University of Missouri - Rolla in September 1958. He received a Bachelor of Science degree in Physics, in June 1962, and a Master of Science degree in Physics, in June 1964, both from the University of Missouri - Rolla, in Rolla, Missouri.

He was enrolled in the Graduate School of the University of Missouri - Rolla as a doctorate candidate from September 1964 to April 1967. In April 1967 he was called to active duty by the U.S. Army as a First Lieutenant in the Ordnance Corps. While in the Army, he served as an instructor with the Defense Atomic Support Agency at Sandia Base, New Mexico. He was released from active duty with the rank of Captain in June 1969. Since his release by the Army he has been enrolled in the Graduate School of the University of Missouri - Rolla.

During the period September 1960 to June 1962 he held four Undergraduate Research Fellowships and a National Defense Education Act Fellowship from September 1962 to June 1965.

The author is married to the former Miss Bernice Uthe of Kansas City, Missouri. They have two daughters, Linda and Patricia, and a son, David.